EXPERIMENTAL INVESTIGATION OF THE IMPACT OF LEEWAY AND RUDDER ANGLES ON THE YAW MOMENT BALANCE FOR WIND-PROPELLED SHIPS

S Hosseinzadeh, D Hudson, S Turnock, M Prince, and **J Banks,** Maritime Engineering Research Group, School of Engineering, University of Southampton, UK

SUMMARY

Wind-assisted propulsion systems are growing in popularity as a technology for decarbonizing maritime transport, due to their capability to lower ships' fuel consumption and mitigate greenhouse gas and other emissions. There is a need, however, to investigate the hydrodynamic implications of wind propulsion for these vessels, particularly the aerodynamic side force causing the hull to adopt a leeway (also known as drift) angle to its heading. The study described in this paper is focused on assessing the hydrodynamic performance of wind-assisted ships under different leeway and rudder angles conditions. A set of self-propelled captive model tests is carried out on the single-screw KCS containership vessel in the University of Southampton's Boldrewood towing tank. The experiments are conducted in an offloaded propeller condition to represent a proportion of the required thrust coming from the wind. A range of leeway angles between ±5° are tested along with a series of rudder angles, varying from -30° to +30° with 10° increments.

A detailed discussion is provided on how varying leeway and rudder angles affect both ship resistance and lateral forces. In addition, the effect of rudder and leeway angles on the yaw moment is studied. The results indicate that as the rudder angle increases, there is a corresponding increase in ship resistance, side force, and rudder-induced yaw moment. For each leeway angle tested the required rudder angle to balance the hydrodynamic induced yaw moment is presented, demonstrating that significant rudder angles may be required for wind propelled ships.

1. INTRODUCTION

The maritime industry faces a challenge in light of the International Maritime Organization's (IMO) updated strategy [1] on decarbonization and zero greenhouse gas (GHG) emissions. This strategy necessitates urgent action from the shipbuilding industry to develop and implement innovative solutions. Among the various methods proposed to mitigate ships' GHG emissions, wind-powered devices have emerged as one of the most promising strategies to reduce fuel consumption and environmental impact of the merchant fleet [2-5]. Modern sail technologies offer a unique advantage in that they are both accessible in the short term and versatile in application. These technologies can be integrated into newly constructed vessels or retrofitted onto existing ships, providing flexibility for widespread adoption across the maritime industry. The potential impact of wind power is substantial, with studies indicating a reduction in fuel consumption ranging from 8% to 48% [6-12], positioning this technology as a promising solution for achieving meaningful reductions in the GHG emissions.

Although wind-assisted propulsion systems offer significant potential for reducing emissions in the shipping industry, their implementation introduces complex challenges for ship designers and naval architects. These systems, though effective in reducing required propeller thrust, generate high aerodynamic side forces on the hull, causing the vessel to operate at an angle of drift. This drift angle not only affects the ship's course but also introduces additional hydrodynamic complexities. The aerodynamic side forces induce both heel and yaw moments on the hull, necessitating a delicate balance between hydrodynamic and aerodynamic forces and moments to maintain a steady heading and direction. Achieving this equilibrium requires sophisticated design considerations and potentially new control systems. These hydrodynamic effects extend beyond simple force balancing. The changed flow regime around the hull can affect the vessel's resistance characteristics, potentially altering its speed-power relationship. The propeller's performance may also be impacted, as it operates in a non-uniform wake field induced by the drift angle. Additionally, the rudder's effectiveness in maintaining course stability may be compromised, requiring careful analysis and possibly design modifications. Moreover, the complex interactions between the hull, propeller, rudder, and their surrounding fluid under drift conditions demand advanced computational and experimental methods to capture with reasonable accuracy. This requirement poses significant challenges in predicting vessel performance and optimizing designs for various operational conditions.

Accurate assessment of fuel savings from wind-assisted propulsion systems necessitates a comprehensive analysis of the ship's thrust, drift, and yaw characteristics. Moreover, precise performance prediction of these vessels requires careful consideration of two critical factors: the added resistance generated by rudder actions to counteract sail-induced yaw moments, and the added resistance resulting from drift caused by substantial side forces. A key challenge in this evaluation lies in accurately quantifying the complex interaction between aerodynamic effects and hydrodynamic behaviour when ships operate at a drift angle [13-16]. Kramer et al., [8] investigated the impact of drift forces on ship resistance, comparing wingsails and Flettner rotors. Their findings revealed that oversimplified models can lead to inaccurate estimations of drift-induced forces. Furthermore, they determined that Flettner rotors exhibit higher side force to thrust ratios and generate more drift-related added resistance compared to wingsails. Kramer et al. [17] conducted experimental research on the effects of drift angle on drag, lift, and yaw moment using ship-like foil geometries. They varied aspect ratios and bottom edge shapes in their experiments. Upon comparing their experimental data with simplified models of lift and lift-induced drag, they concluded that slender body theory fails to accurately predict these forces. Tillig and Ringsberg, [4] employed a ship performance model to assess generic cargo ships, emphasizing the importance of considering interaction effects between sails on wind-powered vessels. Their results highlighted significant discrepancies in predicted lift and drag when using empirical methods. Importantly, they concluded that accurately predicting the lift-to-drag relationship of a ship hull at drift angles is more crucial than precisely determining the drift angle itself.

A review of existing literature reveals significant gaps in our understanding of modern sail technology and its impact on wind-powered vessel performance. While previous studies have predominantly focused on the effects of rudder angles on the hull, this narrow scope fails to provide a comprehensive understanding of the complex interactions at the vessel's stern, particularly between the propulsion system and wake flow. Experimental studies offer valuable insights into wind-powered propulsion systems, yet they present unique challenges that must be carefully considered. A primary concern is the conflicting scaling requirements: traditional ship model tests adhere to Froude scaling laws to accurately represent ship hydrodynamics, whereas wind-assisted vessels also require Reynolds number similarity. In practice, simultaneous adherence to both Froude and Reynolds scaling is unfeasible. Furthermore, the technical challenges associated with generating a representative wind field in a towing tank compound these difficulties. Bordogna et al. [18] addressed some of these challenges by analyzing the Reynolds number effect on the aerodynamic performance of wind-assisted vessels. Their approach involved a series of wind tunnel experiments on a Flettner rotor, although it did not account for hydrodynamic effects. In response to these limitations, Sauder and Alterskjær [19] pioneered a novel cyber-physical empirical method, initially developed for testing floating wind turbines. This approach incorporates wind loads derived from prior numerical analyses into real-time ship motions. While this method offers distinct advantages, the authors acknowledged that their simplified aerodynamic model neglected crucial sail-hull and sail-sail interactions. Moreover, they noted that the semi-empirical equations used for lift and drag coefficients of rotor sails introduced significant uncertainties. Despite these limitations, they emphasized that the cyber-physical approach enables comprehensive validation of new designs and facilitates rapid comparative assessments of various sail types [19].

Despite advancements in computational methods, experimental data remains crucial for validating numerical simulations [12, 20, 21] and assessing the accuracy of performance prediction models in the field of wind-assisted vessels. The complex hydrodynamics of these vessels, particularly the effects of varying leeway angles on hydrodynamic loads and overall ship performance, warrant further in-depth investigation. Experimental data offers a tangible means to verify computational results, identify discrepancies, and ultimately enhance the fidelity of predictive models. Furthermore, systematic experimental studies can reveal unforeseen phenomena or interactions that might be overlooked in purely theoretical or computational approaches. In light of these considerations, the present study focuses on critical aspects of wind-assisted vessel hydrodynamics using experimental methods. Specifically, this research investigates the effects of various leeway angles on hull forces and moments, providing a comprehensive understanding of how these parameters influence the vessel's hydrodynamic behaviour and overall performance. Additionally, it assesses the individual side forces generated by the hull and rudder of a wind-powered ship, offering insights into the distribution of lateral forces and their implications for vessel control and stability.

2. EXPERIMENTAL METHOD

To study the effect of leeway angle on the hydrodynamics of wind-assisted vessels, a series of experiments was conducted in the University of Southampton's Boldrewood towing tank [22]. This state-of-the-art facility measures 138 m in length, 6 m in width, and 3.5 m in depth, with a maximum carriage speed capability of 10 m/s, providing an ideal environment for high-fidelity hydrodynamic testing. The experimental setup utilized

a scaled model of the KRISO Container Ship (KCS) hull form, constructed at a scale ratio of 1:60.96. This model, hereafter referred to as the UoS model, was equipped with a NACA 0018 profile rudder and a high-quality finished titanium alloy KP505 propeller, both scaled accordingly to ensure accurate representation of hull-propeller-rudder interactions. To ensure proper simulation of turbulent flow conditions, a series of standard studs were mounted at 5% of the model's length from the bow.

Table 1 provides detailed specifications of the self-propelled model's main particulars. Figure 1 presents a visual representation of the model, complete with its appendages, and illustrates the test setup configuration. A notable feature of the experimental design was the implementation of a two-post setup to facilitate testing at various leeway angles. The model was secured to the tank carriage at two points: the main post, positioned 2.5 m from the stern, and a secondary post, located 1.5 m from the stern. This configuration established the yaw pivot point, crucial for creating the desired drift angle, at a distance of 2.0 m from the stern, precisely at the midpoint between the two posts. This carefully designed experimental setup allows for a systematic investigation of the hydrodynamic effects of leeway angles on wind-assisted vessels, providing useful insights into the complex interactions between hull, propeller, and rudder under various operating conditions.

Table 1. Main particulars of KCS hull [23].

Parameters	**Full-Scale**	**UoS Model**
Scale (λ)	1	60.96
Displacement (tonne)	52030	0.230
Depth (m)	19.0	0.312
Breadth (m)	32.2	0.528
LBP (m)	230	3.773
LWL (m)	232.5	3.814
Draft Amidships (m)	10.8	0.177
KCS Rudder	NACA 0018	
Wetted Area Rudder (m^2)	115	0.031
Wetted Surface Area (hull+rudder) (m^2)	9539	2.567
Propeller	KP505 (NACA 66) 5 blade	
Propeller Diameter (m)	7.9	0.13
A_e/A_o	0.8	0.8
Propeller rotation direction (from stern)	clockwise	clockwise

As stated, the experimental setup incorporates a twin-post system, implemented through a custom-manufactured plate fitted to the model. This plate, mounted on the carriage centreline, enables precise adjustment of leeway angles within a range of ±8 degrees, with incremental adjustments as fine as 0.5 degrees. The system comprises two interconnected plates: an upper plate attached to the carriage's two posts, and a lower plate directly installed on the model. Both plates are designed to rotate around a pivot point on the model, allowing controlled rotation of the entire model relative to the two posts. This design facilitates secure attachment of the model to the upper plate through a series of matched holes, ensuring stability and accuracy during testing. For these experiments, a single-piece all-movable rudder was used that maintained the same planform as the original semi-balanced skeg rudder. Rudder angle adjustments were achieved using a remotely controlled system, which used thorough calibration prior to the experiments. This calibration process yielded corrected values for each rudder angle, enhancing the precision of the experimental data. The details of the experimental setup are presented in [23].

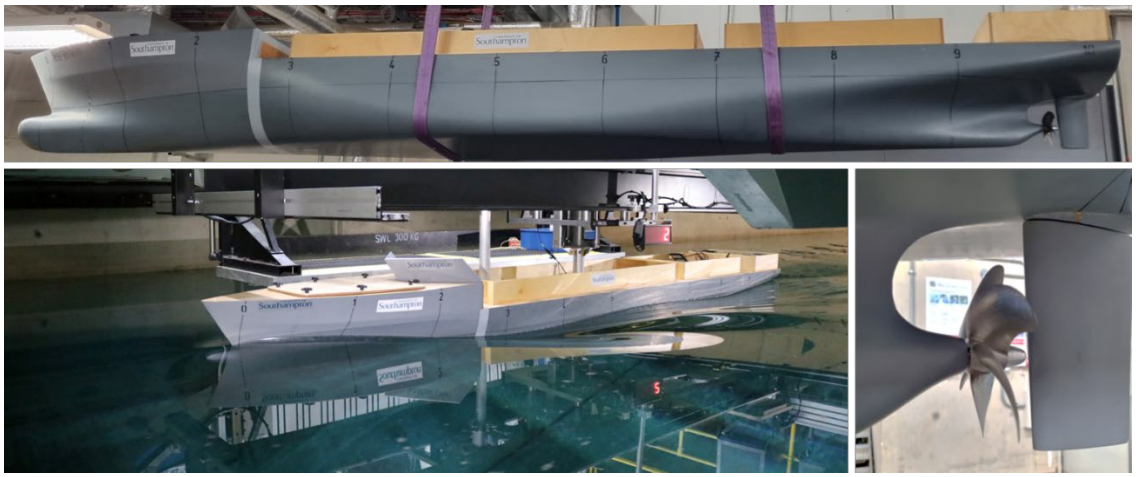

Figure 1: UoS self-propelled model with appendages.

Table 2 provides an overview of the test plan executed in these experiments. The experimental procedure involved setting the desired leeway angle and verifying the functionality of all sensors before proceeding with each test run according to the test matrix. The study encompassed a total of 56 runs, exploring 7 leeway angles, 7 rudder angles, and 4 different RPM settings. The table presents the target propeller RPMs; however, it is worth noting that the recorded RPM varied slightly under different conditions. All tests were conducted at a constant model speed of 1.185 m/s, corresponding to a Froude number of 0.195, ensuring comparable hydrodynamic conditions across all runs. Notably, Table 2 indicates that only two runs were dedicated to different rudder angles. This efficient approach allowed for testing all 7 rudder angles within two runs by configuring four rudder angle changes after every 25 meters of tank travel, maintaining the same propeller RPM and leeway angle. During the experiments the average water temperature was recorded at 16.3°C. For data analysis, freshwater properties were calculated following the ITTC - Recommended Procedures [24]. Specifically, the model freshwater density at the tank temperature was determined to be 998.9 kg/m³, while the model freshwater kinematic viscosity at the tank temperature was calculated as 1.1007E-06 m²/s.

Table 2. Test plan of the self-propelled model experiments.

V_m (m/s)	**Leeway angle (deg.)**	**Rudder angle (deg.)**	**Target Propeller RPM**
1.186	-5 -2.5 -1 0 1 2.5 5	-30 -20 -10 0 10 20 30	$RPM_1 = 448$ $RPM_2 = 554$ $RPM_3 = 644$ $RPM_4 = 768$
Total	7	2	4
Total runs		56	

To collect the experimental data, a specialized software called Lasso, developed by the Wolfson Unit for Marine Technology and Industrial Aerodynamics (WUMTIA) was employed. This software facilitated the comprehensive acquisition of crucial measurements throughout the testing process. The experimental setup allowed for the measurement of multiple parameters simultaneously. At the main post, we recorded the model's drag, heave, trim, and forward side force. Concurrently, the aft side force was measured from the second post. A dedicated rudder dynamometer captured the rudder forces and moments. To evaluate rudder performance comprehensively, a specialized rudder dynamometer was used. This instrument provided six distinct signal outputs, corresponding to various force and moment components of the rudder. The model's propulsion system consisted of a built-in electric motor, enabling the accurate measurement of essential performance metrics such as torque, thrust, and shaft RPM. This setup allowed for a thorough evaluation of the system's effectiveness and efficiency under various test conditions. During the testing phase, data was collected across a total of 16 channels. After each run, the Lasso software was utilized to assess data

consistency before proceeding to the next run, ensuring the integrity and reliability of the collected information. It is important to note that the main data was recorded in the tank axis system, following the right-hand rule with the y-axis pointing to port of the model. In contrast, the rudder dynamometer recorded data in the ship axis system. This distinction in coordinate systems is crucial for accurate data interpretation and analysis.

3. RESULTS AND DSCUSSIONS

This section presents the experimental results and discusses the effects of various parameters on the characteristics of wind-assisted ships. As previously described, experiments were conducted under different propeller conditions at various leeway and rudder angles. To investigate the impact of rudder and leeway angles on the model's total resistance, the results are presented for different configurations. In this study, the drag force, side force, and yaw moment were non-dimensionalized to facilitate a more comprehensive analysis and comparison of the experimental data. Figure 2 illustrates the model's total tow force coefficient (C_T) as a function of rudder angle for different propeller speeds and three leeway angles (β). The total tow force coefficient is defined as $C_T = F_x/(0.5\rho A_w V_m^2)$, where F_x is the measured towing force, ρ is the density of water, A_w is the model's wetted surface area (including both the hull and rudder), and V_m is the model speed. The propeller speed was preset using a remote controller during the experiments, with the details of each run's RPM provided in Table 2.

Several key observations can be made from the presented data. As expected, the total drag increases with increasing rudder angle, regardless of its direction. This trend is consistent across all propeller speeds and leeway angles, likely due to the increased form drag and induced drag associated with larger rudder angles. In addition, increasing propeller speed generally results in lower resistance coefficients. This phenomenon can be attributed to the thrust generated by the propeller, which partially counteracts the total tow force experienced by the model. The total tow force of the model increases with increasing leeway angles. This effect is more pronounced for negative leeway angles, particularly at larger rudder angle. This asymmetry may be due to the complex flow field around the transom of the model and the interaction between the drift-induced flow and the rudder. Furthermore, the resistance curves display a slight asymmetry about the zero-rudder angle, especially for non-zero leeway angles. This asymmetry is likely a consequence of the single-screw propeller configuration, which creates an asymmetric flow field around the propeller and affects the rudder's performance. These observations underscore the complicated relationships between rudder angle, propeller speed, and leeway angle in determining the total tow force of wind-assisted vessels.

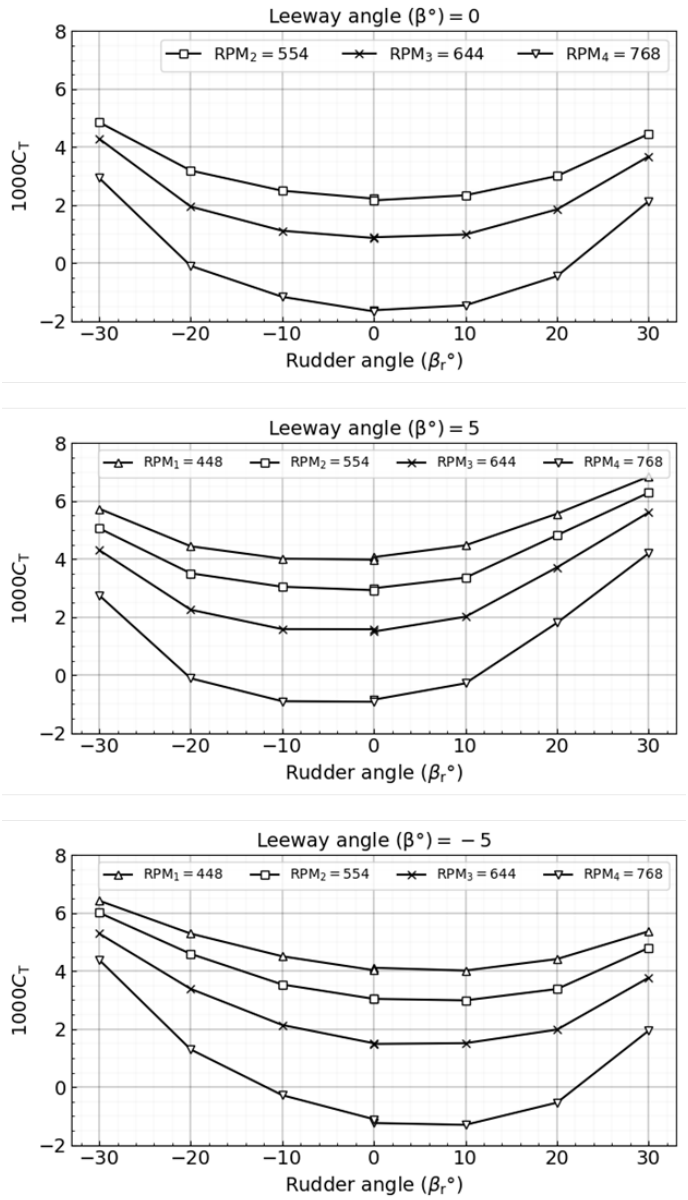

Figure 2: Effect of rudder angle and propeller speed on the model's total tow force coefficient (F_x), presented at three different leeway angles and target propeller RPMs (which varied slightly under different conditions).

The appended hull resistance tests (conducted without the propeller) were also carried out to assess the added resistance introduced by varying leeway angles. To further analyze the drift-induced resistance of the model, Figure 3 presents a comparison of the differences in total tow force coefficient between non-zero and zero leeway angles at zero rudder angle for the non-self-propelled case. In this figure, ΔC_T represents the incremental change in total tow force coefficient relative to the zero-leeway angle condition. As expected, the added resistance due to leeway angle increases with increasing leeway angle. This trend can be attributed to several hydrodynamic factors. Firstly, as the leeway angle increases, the effective angle of attack of the hull increases, leading to a larger pressure differential between the windward and leeward sides of the vessel. This pressure imbalance results in increased form drag. Secondly, the increased leeway angle generates stronger vortices along the hull and at the keel, intensifying the induced drag component. Moreover, the relationship between ΔC_T and leeway angle appears to be non-linear, with the rate of increase in added resistance becoming more pronounced at larger leeway angles. This non-linearity suggests a complex interaction between the hull geometry and the surrounding flow field, possibly involving flow separation and vortex shedding phenomena at higher drift angles. It is worth noting that the observed trends in drift-induced resistance have significant implications for the overall performance and efficiency of wind-assisted vessels. In practical operations,

minimizing leeway angle would be beneficial for reducing the total tow force. However, this must be balanced against the need for lateral force generation in sailing conditions.

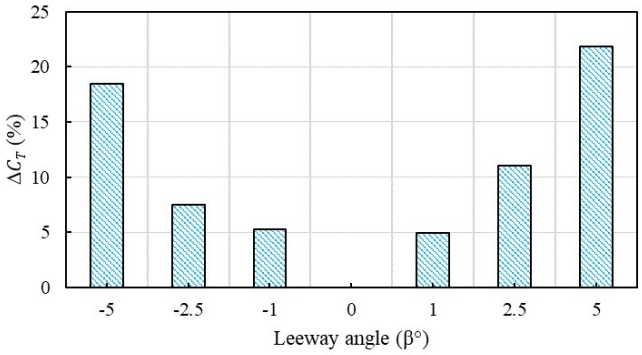

Figure 3: Differences in total tow force coefficient between non-zero and zero leeway angles at zero rudder angle for non-self-propelled case.

Figure 4 presents an analysis of the model's side force, offering important insights into the hydrodynamic performance of wind-assisted vessels. The figure displays the side force coefficient ($C_S = F_y/(0.5\rho A_w V_m^2)$) as a function of rudder angle for different propeller speeds and leeway angles (β). The results reveal several important trends. Generally, as the rudder angle increases in magnitude (both positive and negative), there is a corresponding increase in the side force coefficient of the model. This behavior is expected, as the rudder generating lift (side force) proportional to its angle of attack. The relationship between rudder angle and side force appears to be approximately linear for small to moderate rudder angles. However, a notable departure from this trend occurs at high rudder angles, particularly beyond ±20 degrees. At these extreme angles, the rate of increase in the side force diminishes, and in some cases, the force may even decrease. This phenomenon can be attributed to rudder stall, where flow separation occurs on the rudder's surface, leading to a loss of lift and an increase in drag.

The influence of propeller speed (RPM) on the side force coefficient is also evident. Higher propeller speeds generally result in larger side force coefficients for a given rudder angle. This effect is likely due to the increased flow velocity over the rudder surface induced by the propeller, enhancing its effectiveness. The leeway angle significantly impacts the side force characteristics. At β = 0°, the curves are relatively symmetrical about the zero-rudder angle. However, for non-zero leeway angles (β = 5° and -5°), there is a noticeable shift in the curves. This shift indicates that the hull itself generates a side force when at a leeway angle, which combines with the rudder-induced force to produce the total side force on the vessel.

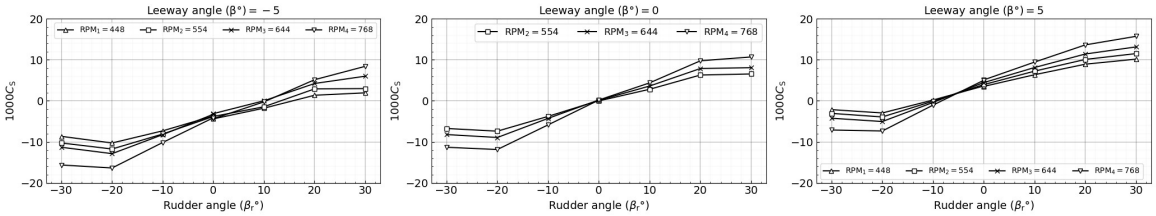

Figure 4: Effect of rudder angle and propeller speed on the model's side force, shown at three different leeway angles and target propeller RPMs (which varied slightly under different conditions).

To gain a more detailed understanding of the hydrodynamic performance of wind-assisted vessels, it is crucial to present results at the ship's self-propulsion point. This approach provides a realistic, accurate, and practical assessment of wind-assisted ship performance, which is invaluable for both design and operational considerations. In this study, we determined the self-propulsion point using the load-varying method at constant speed, following ITTC procedures [25]. The skin friction correction force, denoted as F_D, was calculated based on these procedures. This force accounts for the difference in frictional resistance between the model and full-scale ship due to the Reynolds number effect. Our experimental procedure was as follows: Before each run, we set the selected model speed and propeller loading, then measured the towing force. A range of propeller RPMs were tested, ensuring a range of conditions that would encompass the ship self-

propulsion point and reduced propeller loading conditions that can reflect direct thrust from wind propulsion. Subsequently, we estimated key parameters such as propeller thrust, torque, and side force at the ship's self-propulsion point using spline interpolation of the collected data.

To make our analysis more applicable to real-world scenarios of wind-assisted ships, we present our data in terms of the percentage of propulsion provided by wind. For instance, a "20% wind condition" indicates that we assume 20% of the total required thrust is generated by wind assistance. Therefore, the results throughout the rest of the paper are presented under different wind conditions rather than varying propeller speeds. This approach allows for a deeper understanding of how varying levels of wind assistance affect the vessel's hydrodynamic performance. By analyzing the data in this manner, we can observe how the balance between conventional propulsion and wind assistance impacts various aspects of ship performance. This includes changes in resistance, propeller efficiency, rudder effectiveness, and overall power requirements. Such insights are particularly valuable for optimizing the design and operation of wind-assisted vessels across different wind conditions and sailing routes. Furthermore, it allows for a more accurate assessment of the potential benefits of wind assistance in various operational scenarios, helping shipowners and operators make informed decisions about implementing these technologies.

The side force coefficient (C_S) at 20% thrust from the wind condition across a range of leeway and rudder angles is illustrated in Figure 5. The figure effectively showcases the combined effects of rudder and leeway angles on the side force. As initially noted, there is a clear interaction between rudder angle and leeway angle. The plot exhibits approximate symmetry around the 0° leeway angle, particularly for the extreme rudder angles (-20° and 20°), suggesting that the hull and rudder configuration respond similarly to port and starboard leeway, which is important for balanced ship handling. Notably, rudder angle appears to have a more substantial impact on side force than leeway angle, with changes due to rudder angle variations being more pronounced than those due to leeway angle variations. The relationship between leeway angle and side force is not linear, particularly at extreme rudder angles, which is crucial for understanding ship behavior in various conditions. Even at 0° rudder angle, there's a noticeable change in the side force with varying leeway angles, indicating that the hull itself generates significant side forces when at a leeway angle, even without rudder input. This data reveals that for certain operational requirements, specific combinations of rudder and leeway angles may be more efficient. Given that this data is for 20% wind condition, it's important to note that the generated side forces are a combination of both hydrodynamic effects and the influence of wind on the vessel, likely contributing to the overall trends observed. The data suggests that in wind-assisted navigation, careful management of rudder angle can compensate for leeway-induced side forces, allowing for more precise course-keeping. This information is valuable for optimizing hull and rudder design for wind-assisted vessels, as it clearly shows the complex interaction between these factors in realistic operating conditions.

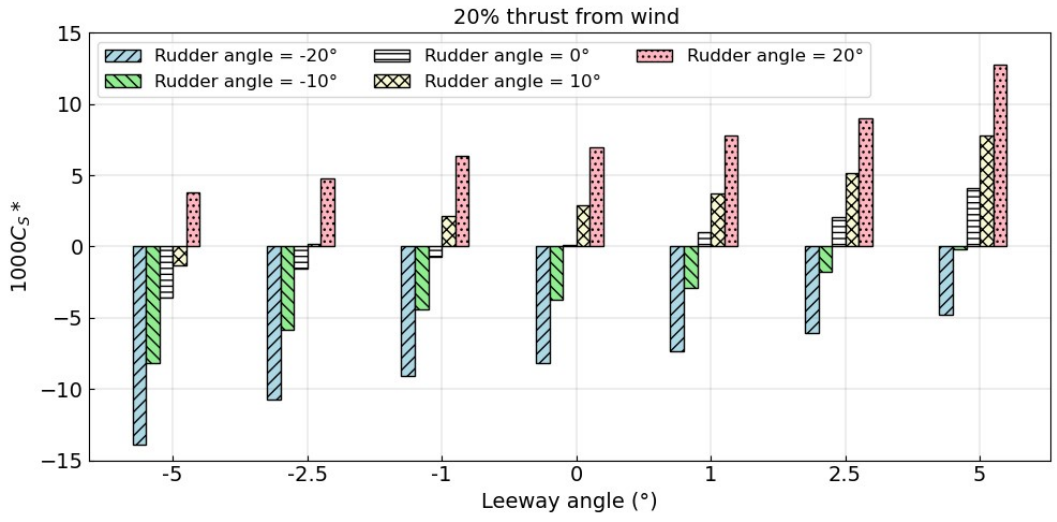

Figure 5: Effect of combined rudder and leeway angles on the model's side force coefficient at 20% thrust from the wind condition.

Figure 6 illustrates the yaw moment coefficient (C_N) at 20% thrust from the wind condition across various leeway and rudder angles. It is shown that, for a given rudder angle, increasing the magnitude of the leeway angle generally results in an increase in yaw moment. This relationship is particularly pronounced at extreme

rudder angles. The subplot in Figure 6, representing the yaw moment at +5° leeway angle across different rudder angles, serves as an excellent example of how rudder angle can be used to counteract the yaw moment induced by leeway. The line intersects the zero-yaw moment axis (shown with a red marker), indicating the rudder angle required to balance the ship at this particular leeway angle. This intersection point is crucial for understanding the rudder angle needed for course-keeping in wind-assisted propulsion scenarios.

Figure 7 expands on this concept by presenting the required rudder angle to balance the hydrodynamic-induced yaw moment for different wind assistance percentages (0%, 20%, and 40%). This figure provides valuable insights into the operational implications of increasing wind assistance. As observed, higher wind percentages generally necessitate slightly larger rudder angles to maintain balance, especially at more extreme leeway angles. The relationship between leeway angle and required rudder angle is notably non-linear, with the curve becoming steeper at higher leeway angles. This non-linearity is consistent across all wind percentages, suggesting a fundamental hydrodynamic principle. While increasing wind percentage does result in larger required rudder angles, the difference is relatively small. This suggests that the hull and rudder design remain effective even with significant wind assistance. These results have significant operational implications, highlighting the importance of active rudder management in wind-assisted ships. From a design perspective, these findings emphasize the need for robust rudder designs in wind-assisted vessels. The rudder must be capable of generating sufficient force to counteract the moments induced by both leeway and wind assistance. It should be highlighted that the yaw balance of the vessel will be affected by the aerodynamic loads and therefore the position of any wind propulsion device should be selected to reduce the required rudder angles.

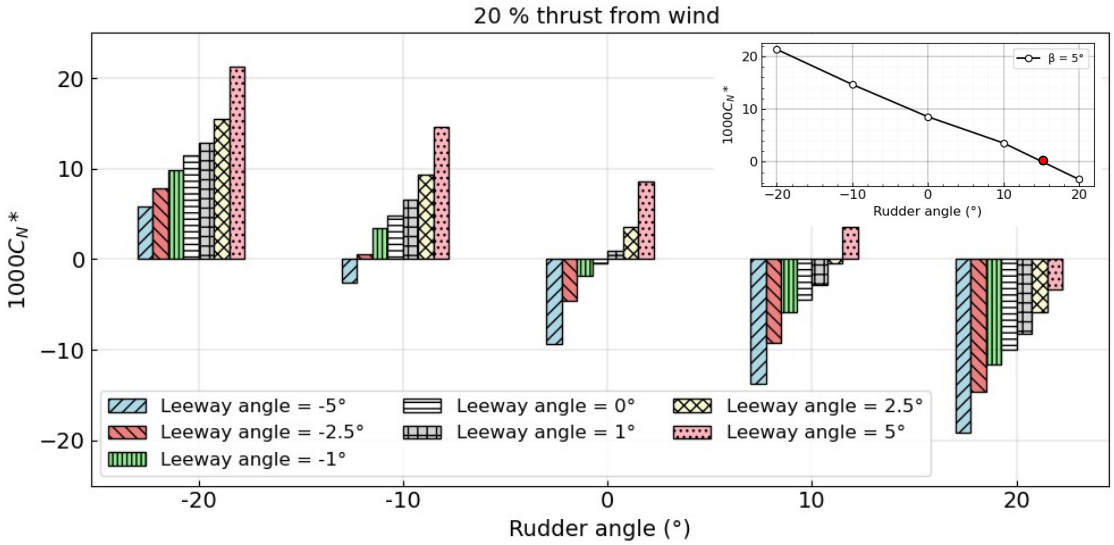

Figure 6: Effect of combined rudder and leeway angles on the yaw moment coefficient at 20% thrust from the wind condition.

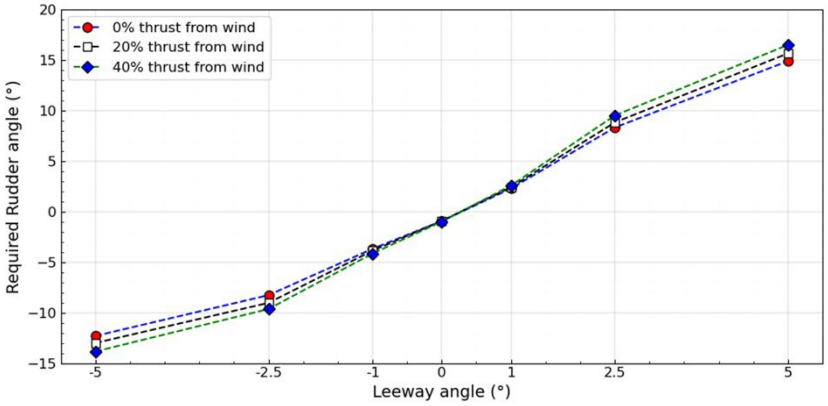

Figure 7: Required rudder angle as a function of leeway angle for different wind conditions.

4. CONCLUSIONS

This study presented an investigation into the hydrodynamic performance of wind-propelled vessels under various rudder and leeway angle conditions. Using a self-propelled KCS model, we experimentally studied the complex interactions between hull, rudder, and propeller, providing valuable insights into the behavior of wind-assisted ships. Our findings revealed the intricate relationships between rudder angle, leeway angle, and wind assistance levels. The total tow force coefficient of the model was found to increase with both rudder angle magnitude and leeway angle, with the effect being more pronounced at negative leeway angles. This asymmetry highlights the importance of considering flow field dynamics, particularly around the transom and propeller. In addition, we analyzed the added resistance caused by the leeway angle, referred to as drift-induced resistance in non-self-propelled scenarios, and demonstrated a 22% increase in the total tow force coefficient for a +5° leeway angle. This analysis provides crucial data for understanding the efficiency trade-offs in wind-assisted propulsion.

The side force coefficient analysis demonstrated a clear interaction between rudder and leeway angles. For instance, at positive rudder angles, increasing leeway angle from negative to positive values generally increased side force, while the opposite trend was observed for negative rudder angles. This interaction is crucial for understanding ship manoeuvrability and course-keeping abilities in wind-assisted conditions. Our analysis of yaw moment revealed that increasing leeway angle magnitude results in greater yaw moment, necessitating larger rudder angles for balance. Importantly, while reduced thrust loading required slightly larger rudder angles to maintain equilibrium, the difference was not substantial, suggesting that the rudder efficiency was not significantly affected.

In conclusion, this study provides a solid foundation for understanding the hydrodynamic challenges and opportunities presented by wind-assisted propulsion in modern shipping. As the maritime industry continues to seek more sustainable propulsion methods, the insights gained from this research will be instrumental in developing efficient, reliable, and environmentally friendly wind-assisted vessels. The present findings contribute substantially to the development of performance prediction algorithms for such ships, offering a foundation for more accurate modeling and optimization of wind-assisted vessels. Future studies could further develop these findings by investigating propeller efficiency in wind-assisted vessels, as this remains a critical factor in overall ship performance. Additionally, research into the long-term operational aspects, including fuel savings and economic viability, would provide valuable insights for the practical implementation of wind-assisted propulsion technologies.

5. ACKNOWLEDGEMENTS

This work was conducted as part of the Winds of Change Clean Maritime Demonstration project funded by UKShore and Innovate UK. The authors acknowledge the staff at the Wolfson Unit MTIA, for their crucial role greatly contributed to the preparation of our experiments. The author further expresses gratitude to the dedicated staff at the Boldrewood Towing Tank at the University of Southampton, David Turner and Rodolfo Olvera, for their invaluable support throughout this experimental study.

6. REFERENCES

1. International Maritime Organization, ‘IMO strategy on reduction of GHG emissions from ships, Technical report’, Marine Environment Protection Committee, *International Maritime Organization*, 2023.

2. PETKOVIC, M., et al., ‘Wind Assisted Ship Propulsion Technologies Can they Help in Emissions Reduction?’ *NAŠE MORE: znanstveni časopis za more i pomorstvo*, 68(2): p. 102-109, 2021.

3. KHAN, L., et al., ‘A review of wind-assisted ship propulsion for sustainable commercial shipping: latest developments and future stakes’, *Royal Institution of Naval Architects (RINA)*, 2021.

4. TILLIG, F., and RINGSBERG, J W., ‘Design, operation and analysis of wind-assisted cargo ships’, *Ocean engineering*, 211: p. 107603, 2020.

5. ARABNEJAD, M H., et al., ‘Zero-emission propulsion system featuring, Flettner rotors, batteries and fuel cells, for a merchant ship’, *Ocean Engineering*, 310: p. 118618, 2024.

6. OUCHI, K., et al, ‘Wind challenger” the next generation hybrid sailing vessel’, in *The Third International Symposium on Marine Propulsors, Launceston, Tasmania, Australia*. 2013.

7. TILLIG, F., et al., ‘Reduced environmental impact of marine transport through speed reduction and wind assisted propulsion’, *Transportation Research Part D: Transport and Environment*, 83: p. 102380, 2020.

8. KRAMER, J A., STEEN, S., and SAVIO, L., ‘Drift forces—Wingsails vs. Flettner rotors’, in *Proceedings of the International Conference on High Performance Marine Vehicles, Cortona, Italy*, 2016.

9. VÄINÄMÖ, J., ‘Operational Experiences and Results from the First Reference Installation from Nov-2014 Roro-Ship Estraden (9700 Dwt)’, in *24th International HISWA Symposium on Yacht Design and Yacht Construction. Amsterdam, The Netherlands*, 2016.

10. LU, R., and RINGSBERG, J W., ‘Ship energy performance study of three wind-assisted ship propulsion technologies including a parametric study of the Flettner rotor technology’, *Ships and Offshore Structures*, 15(3): p. 249-258, 2020.

11. AMMAR, N R., and SEDDIEK, I S., ‘Wind assisted propulsion system onboard ships: case study Flettner rotors’, *Ships and Offshore Structures*, 17(7): p. 1616-1627, 2022.

12. KRAMER, J V., and STEEN, S., ‘Simplified test program for hydrodynamic CFD simulations of wind-powered cargo ships’, *Ocean Engineering*, 244: p. 110297, 2022.

13. VIOLA, I M., et al., ‘A numerical method for the design of ships with wind-assisted propulsion’, *Ocean Engineering*, 105: p. 33-42, 2015.

14. LEE, H., et al., ‘Surrogate model based design optimization of multiple wing sails considering flow interaction effect’, *Ocean Engineering*, 121: p. 422-436, 2016.

15. TILLIG, F., et al., ‘Analysis of uncertainties in the prediction of ships’ fuel consumption–from early design to operation conditions’, *Ships and Offshore Structures*, 13(sup1): p. 13-24, 2018.

16. VAN DER KOLK, N., et al., ‘Case study: wind-assisted ship propulsion performance prediction, routing, and economic modelling’, in *International Conference Power & Propulsion Alternatives for Ships. The Royal Institution of Naval Architects (RINA)*, 2019.

17. KRAMER, J A., STEEN, S., and SAVIO, L., ‘Experimental study of the effect of drift angle on a ship-like foil with varying aspect ratio and bottom edge shape’, *Ocean Engineering*, 121: p. 530-545, 2016.

18. BORDOGNA, G., et al., ‘Experiments on a Flettner rotor at critical and supercritical Reynolds numbers’, *Journal of Wind Engineering and Industrial Aerodynamics*, 188: p. 19-29, 2019.

19. SAUDER, T., and ALTERSKJÆR, S A., ‘Hydrodynamic testing of wind-assisted cargo ships using a cyber–physical method’, *Ocean Engineering*, 243: p. 110206, 2022.

20. ZHANG, Y., et al., ‘Influence of leeway on hull-propeller-rudder interaction using CFD methods’, *Norwegian University of Science and Technology*, 2023.

21. ZHANG, Y., et al., ‘Influence of drift angle on the propulsive efficiency of a fully appended container ship (KCS) using Computational Fluid Dynamics’, *Ocean Engineering*, 292: p. 116537, 2024.

22. MALAS, B., et al., ‘Design, development and commissioning of the Boldrewood towing tank–a decade of endeavour, *International Journal of Maritime Engineering*, 165(A3 (2023)): p. A-255-A-271, 2024.

23. HOSSEINZADEH, S., et al., 'Experimental Dataset of a Model-Scale Ship in Calm Water and Waves', *Available at SSRN 4851029*, 2024, https://dx.doi.org/10.2139/ssrn.4851029.

24. ITTC, Recommended procedures and guidelines: Fresh Water and Seawater Properties, 2011.

25. ITTC. Recommended Procedures and Guidelines, Testing and Extrapolation Methods-Propulsion, Performance Propulsion Test. in *International Towing Tank Conference*, 2008.

7. AUTHORS BIOGRAPHY

Saeed Hosseinzadeh holds the current position of Research Fellow at University of Southampton. He is mainly responsible for conducting experimental studies of wind-propelled vessels and performing hydro/aerodynamic analysis of these vessels using numerical simulations. His previous experience includes analyzing impact-induced loads on elastic structures, conducting flexible fluid-structure interaction analyses, performing seakeeping analysis of high-speed craft, and developing mathematical models for such vessels.

Dominic Hudson holds the current position of Shell Professor of Ship Safety and Efficiency at the University of Southampton. Dominic has research interests in all aspects of hydrodynamics, particularly as related to ship design and operation for energy efficiency. He advises Shell Shipping and Maritime on ship efficiency, decarbonisation, performance management and future ship designs. He is currently working on energy efficient technologies for shipping, including draft and trim optimisation, air lubrication and assessment of wind-assist devices.

Stephen Turnock, FRINA is Professor of Maritime Fluid Dynamics with expertise in: ship energy efficiency and future fuels; marine renewable energy, autonomous systems and performance sport.

Martyn Prince holds the position of Principal Research Engineer at the Wolfson Unit for Marine Technology and Industrial Aerodynamics at the University of Southampton. His primary areas of expertise involve aerodynamic and hydrodynamic experimental testing and sailing (and wind assisted) vessel performance prediction.

Joseph Banks holds the current position of Associate Professor in Maritime Engineering at the University of Southampton. He specialises in experimental and computational fluid dynamics with particular interests in high performance sport, fluid structure interactions and the performance of sailing and wind-assisted ships.